Title

Simulation system for understanding the lag effect in fluoroscopic images

Authors * Corresponding author

Rie Tanaka[1]*, Hiroki Kawashima[2,3], Katsuhiro Ichikawa[1], Kosuke Matsubara[1], Hiroji Iida[3], Shigeru Sanada[1]

Affiliation

[1] School of Health Sciences, College of Medical, Pharmaceutical and Health Sciences, Kanazawa University; 5-11-80 Kodatsuno, Kanazawa, 920-0942 Japan

[2] Division of Health Sciences, Graduate School of Medical Science, Kanazawa University; 5-11-80 Kodatsuno, Kanazawa, 920-0942 Japan

[3] Department of Radiological technology, Kanazawa University Hospital; 13-1 Takara-machi, Kanazawa, 920-8641, Japan

Telephone and Fax numbers and E-mail Address of Corresponding Author

Rie Tanaka, PhD

Tel: +81-76-265-2537

Fax: +81-76-234-4366

E-mail: rie44@mhs.mp.kanazawa-u.ac.jp

Department of Radiological Technology, School of Health Sciences, College of Medical, Pharmaceutical and Health Sciences, Kanazawa University; 5-11-80 Kodatsuno, Kanazawa, 920-0942, Japan

Abstract

Real-time tumor tracking in external radiotherapy can be achieved by diagnostic (kV) X-ray imaging with a dynamic flat-panel detector (FPD). It is crucial to understand the effects of image lag for real-time tumor tracking. Our purpose in this study was to develop a lag simulation system based on the image lag properties of an FPD system. Image lag properties were measured on flat-field images both in direct- and indirect-conversion dynamic FPDs. A moving target with image lag was simulated based on the lag properties in all combinations of FPD types, imaging rates, exposure doses, and target speeds, and then compared with actual moving targets for

investigation of the reproducibility of image lag. Image lag was simulated successfully and agreed well with the actual lag as well as with the predicted effect. In the indirect-conversion FPD, a higher dose caused greater image lag on images. In contrast, there were no significant differences among dose levels in a direct-conversion FPD. There were no relationships between target speed and amount of image blurring in either type of FPD. The maximum contour blurring and the rate of increase in pixel value due to image lag were 1.1 mm and 10.0%, respectively, in all combinations of imaging parameters examined in this study. Blurred boundaries and changes in pixel value due to image lag were estimated under various imaging conditions with use of the simulation system. Our system would be helpful for a better understanding of the effects of image lag in fluoroscopic images.

1. Introduction

Real-time tumor tracking has been facilitated by the use of diagnostic (kV) X-ray imaging with a dynamic flat-panel detector (FPD) in external radiotherapy [1 – 3]. Kilovoltage X-ray imaging is expected to solve the problems of low image contrast and poor image quality seen in megavoltage imaging. However, several factors remain that could reduce the accuracy of target tracking in external radiation therapy. In terms of image quality, it is thought that image lag, ghosting, image noise, and image resolution affect the accuracy of tracking. In particular, a great deal of attention must be paid to image lag—i.e., the carryover of the image charge generated by previous X-ray exposure into subsequent image frames [4,5]—because it may induce blurring on the contours of a moving target.

Previous studies indicated that primary a-Se type of FPDs showed a lag in the first frame after an X-ray exposure of less than 5% of the original signal [6 – 9]. Modifications in a-Se detector technology appear to have resulted in marked decreases in both lag and ghosting effects in more recent systems [10 – 12]. However, the effect of image lag on the accuracy of target tracking has not been fully addressed except for one investigation carried out under restricted conditions of imaging parameters by use of a direct-conversion FPD [13].

In real-time tumor tracking, it is necessary to optimize the imaging parameters in each

patient to keep the patient dose as low as possible while maintaining tracking accuracy. In addition, it is crucial to understand the amount of blurring on the contours of a moving target due to image lag in order to set an appropriate margin around a target when planning radiotherapy. A previous study showed that the amount of image lag could be changed depending on the exposure dose and the type of FPD [14]. If the amount of image blurring on the contours of a moving target could be estimated based on the image lag properties of an FPD system, it would be useful for a margin setting and for parameter selection in radiotherapy planning of real-time target tracking. Thus, we launched a simulation system for understanding the lag effect in fluoroscopic images. We performed this study to develop a lag simulation system that provided image blurring for all parameter settings, such as the exposure dose (mR), target speed (mm/s), imaging rate (frame per sec; fps), and type of FPD.

2. Materials and Methods

2. 1. Measurement of lag properties

Lag measurements were performed with a direct- and an indirect-conversion dynamic FPD, SONIALVISION Safire2 (Shimadzu, Japan) and AXIOM Luminos dRF (Siemens, Germany), according to the IEC 62220-1-3 standard [15]. Fluoroscopic images were obtained at three standard X-ray spectra (IEC RQA3, RQA5, RQA7), at three imaging rates (3.0 fps, 7.5 fps, 15 fps), and at three exposure dose levels at the detector surface (direct-conversion type: 0.05 mR, 0.1 mR, 0.2 mR; indirect-conversion type: 0.01 mR, 0.02 mR, 0.04 mR). The exposure dose was determined according to the IEC62220-1-3 standard [15], although with differences among FPD types due to the difference in imaging mode (direct-conversion type: dynamic imaging mode; indirect-conversion type: fluoroscopic imaging mode). The matrix size was 1024 × 1024 pixels, the pixel size was 300 × 300 µm, the field of view (FOV) was 30.4 × 30.4 cm, and the grayscale range of the images was 16 bits in the direct-conversion FPD. The matrix size was 1024 × 1024 pixels, the pixel size was 130 × 130 µm, the FOV was 15.1 × 15.1 cm, and the grayscale range of the images was 16 bits in the indirect-conversion FPD.

Image lag can be defined as the carryover of trapped charges generated by X-ray exposure into subsequent frames acquired with no X-ray exposure. The lag in the nth frame (L_n) was calculated as follows [4]:

$$, \qquad (1)$$

where S_0 is the average pixel values measured in the region of interest (ROI) in the frame acquired just before X-ray cutoff, and S_n is that acquired in the nth frame after X-ray cutoff. The term B is the pixel value measured in the background image, which

was obtained without any radiation. The details were described elsewhere [14]. Figure 1 shows one of the image lag properties which was installed in our simulation system as initial data. These data were also prepared for the other imaging parameters, i.e., three dose qualities, three dose levels, and three imaging rates.

2. 2. Simulation of a moving target with image lag

2.2.1. Target settings

Our system was designed to provide two types of target, i.e., a digital phantom simulating a round target and a real target cut out from a real radiograph, as shown in Fig. 2.

The digital phantom was created based on a Gaussian distribution as follows:

$$(0 \leq x < S), (0 \leq y < S), \quad (2)$$

where x and y are the distance from the center of the Gaussian distribution, which determine a target size S. The n and r are the number of frames processed and the movement rate in units of pixels/frame, respectively, which control the mean displacement of the target, and σ is a parameter that controls the edge gradient of the target.

The target moving rates were prepared in three patterns, i.e., 10 mm/s, 20 mm/s, and 30 mm/s, covering the moving rates of lung tumors in clinical practice [16]. The target motion was given a user-specified trajectory, which was digitally superimposed onto a flat-field image. The target in the nth frame T(n) is described as

$$\quad (3)$$

where P is the pixel value at the center of the target, for which any value could be set according to the average pixel value of the insert position. The superimposed image was created by addition of T(n) to a plain or original image. We used the digital phantom to calculate predicted values of image lag in this study (Fig. 2a).

Meanwhile, our system provided a real target by clipping out the ROI from a real radiograph. In this study, a simulation lung nodule with a diameter of 1 cm (paraffin mixture) on a 15 cm-thick acrylic plate was imaged by use of the FPD systems under the same conditions as in lag measurements (RQA5, 15 fps, SID = 150 cm). The ROI, 40 mm on a side, was located on the nodule area and clip out for use in a system evaluation in this study (Fig. 2b).

2.2.2. Lag simulation

A moving target in the nth frame, Tlag(n) , was simulated by use of the results of the lag measurement as follows:

, (4)

where k is the frame number going back from the nth frame of interest, and Lk is the image lag (%) calculated by Eq. (1). The computation was repeated, for Lk was greater than 1.0. Here, T(0) means a target without lag, equivalent to a static target.

2.3. Calculation of predicted value

We used the digital phantom, as shown in Fig. 2a, to calculate predicted values. Image lag was simulated by use of the known image lag properties. The effect of image lag was estimated based on the simulation results, at each exposure dose, type of FPD, and target speed.

2.4. System evaluation

2.4.1. Evaluation items

The real target, as shown in Fig. 2b, was used for system evaluation. The system was validated in terms of the reproducibility of image lag, indicating increases in pixel value and image blurring on the contours of a moving target. Previous studies indicated that image lag properties are dependent on the exposure dose and FPD type without relation to the imaging rate and exposure quality. Thus, the validation was conducted in terms of FPD type (direct or indirect), exposure dose (direct-conversion type: 0.05 mR, 0.1 mR, 0.2 mR; indirect-conversion type: 0.01 mR, 0.02 mR, 0.04 mR), and target speed (10 mm/s, 20 mm/s, and 30 mm/s). The target speed was set at 10 mm/s for investigation of differences in exposure dose. In the validation of differences in target speed, the exposure dose was set at reference dose levels, 0.2 mR in the direct-conversion type and 0.04 mR in the indirect-conversion type.

2.4.2. Image acquisition

For the system validation, simulated lag was compared with the actual lag of a real moving target. A simulated lung nodule with a diameter of 1 cm, the same as that used in Section 2.2.1, was mounted onto a motor control device (Servomotor, LINEARCAM YMS-55; Asahi Measurement, Japan), which provided not only a constant velocity, but also arbitrary motion. The simulation nodule was moved in contact with a 15 cm-thick acrylic plate on the detector surface. The motion speed was 10, 20, or 30 mm/s, covering the range of lung tumor movement during normal breathing [16].

2.4.3. Measurement of lag effect

ROIs of 40 × 40 mm2 were located on the lung nodule area and trimmed. Profile curves

were obtained horizontally across the moving target, and the half-value width of the profile curve was measured for quantification of image blurring on the contours of a moving target as the difference in width measured between the static and moving targets. In addition, increases in pixel value due to image lag were calculated as pixel values relative to the maximum original value measured on the static nodule. The results were compared among simulation and actual moving targets, and against each predicted value.

3. Results

3.1. Calculation of predicted value

Figures 3 and 4 show the process of creating a target with image lag, and Fig. 5 shows the resulting images. The motion speed of all targets in Fig. 3 was set at 10 mm/s. The exposure dose of all targets in Figs. 4 was set at reference levels, 0.2 mR in the direct-conversion type and 0.04 mR in the indirect-conversion type. Differences in the effect of image lag were estimated according to the known image lag properties as follows:

(i) In terms of radiation dose, the effect of image lag increases with increases in exposure dose in an indirect-conversion FPD, because the lag effect is dependent on the dose level. In contrast, there is little or no difference among different dose levels in a direct-conversion FPD, because of the independence of image lag on the dose level (Fig. 1, Fig. 3, and Table 1).

(ii) In terms of target speed, the lag effect shows no trend, because of the offset between two factors— slower target motion results in accumulation of more image lag in the same region, whereas faster target motion affects a larger area (Fig. 4 and Table 1).

(iii) In terms of FPD type, almost the same effect is observed in direct and indirect-conversion FPDs, because of the offset between large image lag (%) in a direct-conversion FPD and continuous image lag (%) in an indirect-conversion FPD (Fig. 1).

3.2. System evaluation

Figure 6 shows profile curves of a moving target with actual and simulated lag for each dose level. The profile curves show that pixel values increased with lag in both the actual and simulation targets in comparison to the static targets. Increases in pixel values were also observed for movement in the rearward direction. In particular, increases in pixel value, with the appearance of trailing, were demonstrated at a dose level of 0.04 mR in the indirect-conversion FPD, although it was difficult to find such an

increase due to image noise at lower dose levels. Tables 2 and 3 show the maximum image blurring found on the contours of a moving target at each dose level. In the indirect-conversion FPD, the higher dose showed a greater impact of image lag. In contrast, there were no significant differences among dose levels in the direct-conversion FPD. In general, the increases in the pixel value of the simulation images tended to be larger than those of the actual images. Figure 7 shows the profile curves obtained on the actual and simulation target moving at 10 mm/s, 20 mm/s, and 30 mm/s. Increases in pixel value were observed on the moving target as well as in movement in the rearward direction. Tables 4 and 5 show the maximum image blurring found on the contours of a moving target at each motion rate. The effect of image lag found in the indirect-conversion FPD was larger than that in the direct-conversion FPD. However, there was no relationship between target speed and amount of image blurring in either type of FPD. The maximum contour blurring and increased rate in pixel value due to image lag were less than 1.1 mm and 10.0%, respectively, for all combinations of imaging rate and target motion rate examined in this study.

4. Discussion

Image lag was simulated based on the image lag properties of the system with various combinations of imaging parameters, such as the exposure dose, target motion rate, and type of FPD. The effect of image lag was seen as blurred boundaries of moving targets and was measured quantitatively as increase in the width of the target contour and in the pixel value. It was confirmed that our system simulated image lag appropriately by comparison between the actual and predicted lag.

The effects of image lag increased with increasing exposure dose in an indirect-conversion FPD. This result was supported by the lag properties depending on dose levels. In contrast, there was little difference among different dose levels in a direct-conversion FPD. This was also thought to be an accurate reflection of the lag properties in the direct-conversion FPD. On the other hand, there was no tendency for the effect of image lag at each target speed. The results could be explained by the offset among two factors as expected; the slower target motion resulted in accumulation of more image lag in the same region, whereas faster target motion affected a larger area. In particular, the image lag provided an increase in the base level of the pixel value rather than a decrease in the image resolution in indirect-conversion type FPD, because of sharply decreased but continuous lag with the appearance of tailing. The lag property was thought to be the reason for the lack of influence on the half-value width of targets regardless of variations in target speed. In addition, almost the same effect was

observed in direct and indirect-conversion FPDs. This was thought to be due to the offset between large image lag (%) in a direct-conversion FPD and continuous image lag (%) in an indirect-conversion FPD. The difference in lag properties between the direct [,] and indirect-conversion FPDs is caused by the differences in the physical structures used in the FPDs. It was reported previously that the effect of image lag in an indirect-conversion FPD took a longer time to become less than 1.0% than in a direct-conversion FPD [14,17]. Our results were thought to be an accurate reflection of image lag properties in each type of FPD. The observation that the predicted effect was reflected in the simulated images indicated that our system simulated image lag appropriately. However, we only investigated an FPD in each conversion type only under limited conditions. Thus, further studies are required for characterization of lag properties in each type of FPDs.

The visible contour blurring of a moving target is a potential source of errors in target tracking in external radiotherapy, i.e., leaving the track due to false detection of the target. Thus, our simulation system is expected to be helpful for determination of appropriate margins and imaging conditions according to the properties of the target and imaging system. In fact, the maximum contour blurring and the rate of increase in pixel value due to image lag were less than 1.1 mm and 10.0%, respectively, for all combinations of imaging rate and target motion rate examined in this study. Although image lag has no significant impact on moving target imaging, it might be one of the error factors for target tracking. Furthermore, the maximum image blurring and increase in pixel value were expected to be 1.4 mm and 16%, respectively, in the indirect-conversion FPD according to the predicted values based on the properties of image lag. The predicted values of image lag could have a significant impact on the tracking accuracy. In general, the FPD incorporates measures to minimize lag by use of refresh light, which reconditions the detector prior to each new image acquisition cycle [18]. We need to investigate the effect of the light in each type of FPD. In addition, there are the other influencing factors, such as image contrast, image noise, target background, and some correction mechanisms used in FPD systems, which may affect the accuracy of target tracking in external radiation therapy. In this study, there were some differences in the lag effect between the actual and simulated values. These differences could also be explained by such influencing factors. Thus, further studies are required for investigation of these factors and the effects on the overall spatial uncertainty in external radiotherapy.

5. Conclusion

Blurred boundaries and changes in pixel values due to image lag could be estimated in various imaging situations by use of the image lag simulation system developed in this study. Our simulation indicated that the lag effect depends on exposure dose and FPD type, and the results agreed well between the effects of the actual and predicted lag. Our system will be useful for forwarding a better understanding of the effects of image lag in fluoroscopic imaging.

References
1.   Jaffray DA, Siewerdsen JH, Wong JW, Martinez AA.   Flat-panel cone-beam computed tomography for image-guided radiation therapy. Int J Radiat Oncol Biol Phys 2002;53:1337-1349.
2.   Moore CJ, Amer A, Marchant T, Sykes JR, Davies J, Stratford J, et al. Developments in and experience of kilovoltage X-ray cone beam image-guided radiotherapy. Br J Radiol 2006;79:66-78.
3.   Huntzinger C, Munro P, Johnson S, Miettinen M, Zankowski C, Ahlstrom G, et al. Dynamic targeting image-guided radiotherapy. Med Dosim 2006;31:113-125.
4.   Zhao W, Degrescenzo G, and Rowlands JA. Investigation of lag and ghosting in amorphous selenium flat-panel detectors. SPIE medical imaging 2002, Proc. SPIE 4682:9-20.
5.   Bloomquist AK, Yaffe MJ, Mawdsley GE, Hunter DM, Beideck DJ. Lag and ghosting in a clinical flat-panel selenium digital mammography system. Med Phys 2006;33:2998-3005.
6.   Siewerdsen JH and Jaffray DA. A ghost story: Spatio-temporal response characteristics of an indirect detection flat-panel imager. Med.Phys 1999; 26:1624-1641.
7.   Choquette M, Rougeot H, Martin J, Laperriere L, Shukri Z, and Polischuk B. Direct selenium x-ray detector for fluoloscopy, R&F, and radiography. SPIE medical imaging 2000, Proc. SPIE 3977:128-136.
8.   Adachi S, Hori N, Sato K., Tokuda S, Sato T, Uehara K, et al. Experimental evaluation of a-Se and CdTe flat-panel detectors for digital radiography and fluoroscopy. SPIE medical imaging 2000, Proc. SPIE 3977:38-47.
9.   Schroeder C, Stanescu T, Rathee S, Fallone BG. Lag measurement in an a-Se active matrix flat-panel imager. Med Phys 2004;31:1203-1209.

10.   Pokischuk B, Shukri Z, Legros A, and Rougeot H. Selenium direct converter structure for static and dynamic x-ray detection in medical imaging applications. SPIE medical imaging 1998. Proc. SPIE 3336:494-504.

11.   Lee DL, Cheung LK, Rodricks B, and Powell GF. Improved imaging performance of 14x17-inch direct radiography system using Se/TFT detector. SPIE medical imaging1998, Proc. SPIE. 3336:14-23.

12.   Tsukamoto A, Yamada S, Tomisaki T, Tanaka M, Sakaguchi T, Asahina H, et al. Development and evaluation of a large-area selenium-based flat panel detector for real-time radiography and fluoroscopy. SPIE medical imaging 1999, Proc. SPIE. 3659:14-23.

13.   Tanaka R, Ichikawa K, Mori S, Dobashi S, Kumagai M, Kawashima H, et al. Investigation on effect of image lag in fluoroscopic images obtained with a dynamic flat-panel detector (FPD) on accuracy of target tracking in radiotherapy. JRR 2010;51: 723-731

14.   Kawashima H, Tanaka R, Ichikawa K, Matsubara K, Iida H, Sanada S. Effect of image lag and influencing factor in fluoroscopy images obtained with a dynamic flat-panel detector (FPD), Journal of computer assisted radiology and surgery, 7(1):S60-61,2012.

15.   Determination of the detective quantum efficiency – detectors used in dynamic imaging. In: IEC International standard 62220-1. Medical diagnostic X-ray equipment-Characteristics of digital imaging devices-Part 3 Geneva, International electrotechnical commission; 2008.

16.   West JB. Respiratory Physiology – the Essentials 6th ed. Philadelphia, PA: Lippincott Williams & Wilkinss; 2000:11-19.

17.   Teramoto A, Kajihara T, Suzuki S, Kinoshita K, Tsuzaka M, Fujita H. Development of quality control system for flat-panel detectors. Radiol Phys Technol. 2011;4:164-72.

18.   Cowen AR, Davies AG, Sivananthan MU. The design and imaging characteristics of dynamic, solid-state, flat-panel x-ray image detectors for digital fluoroscopy and fluorography. Clinical Radilogy. 2008;63:1073-1085.
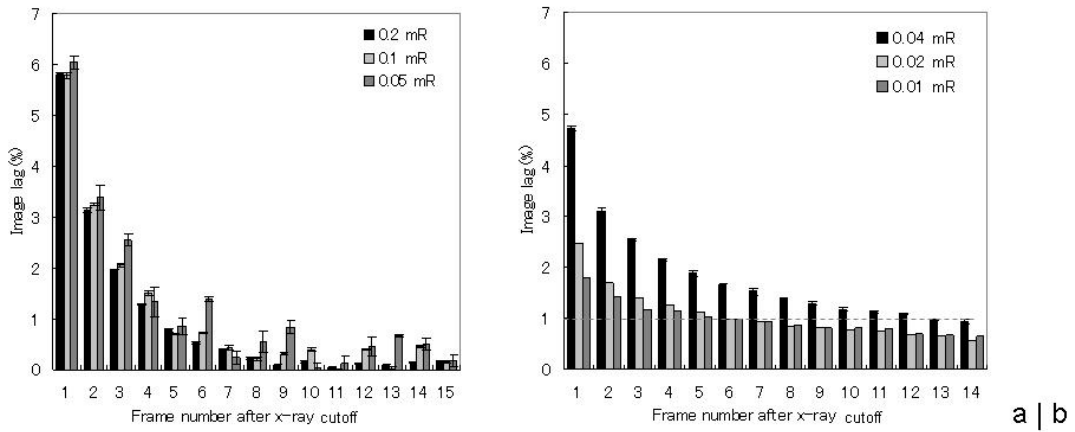
Fig. 1 Image lag properties in our system for (a) direct- and (b) indirect-conversion
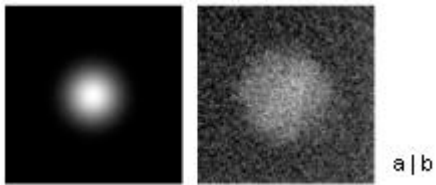
FPDs.

Fig. 2 The two types of target used in our system. (a) A digital phantom simulated round

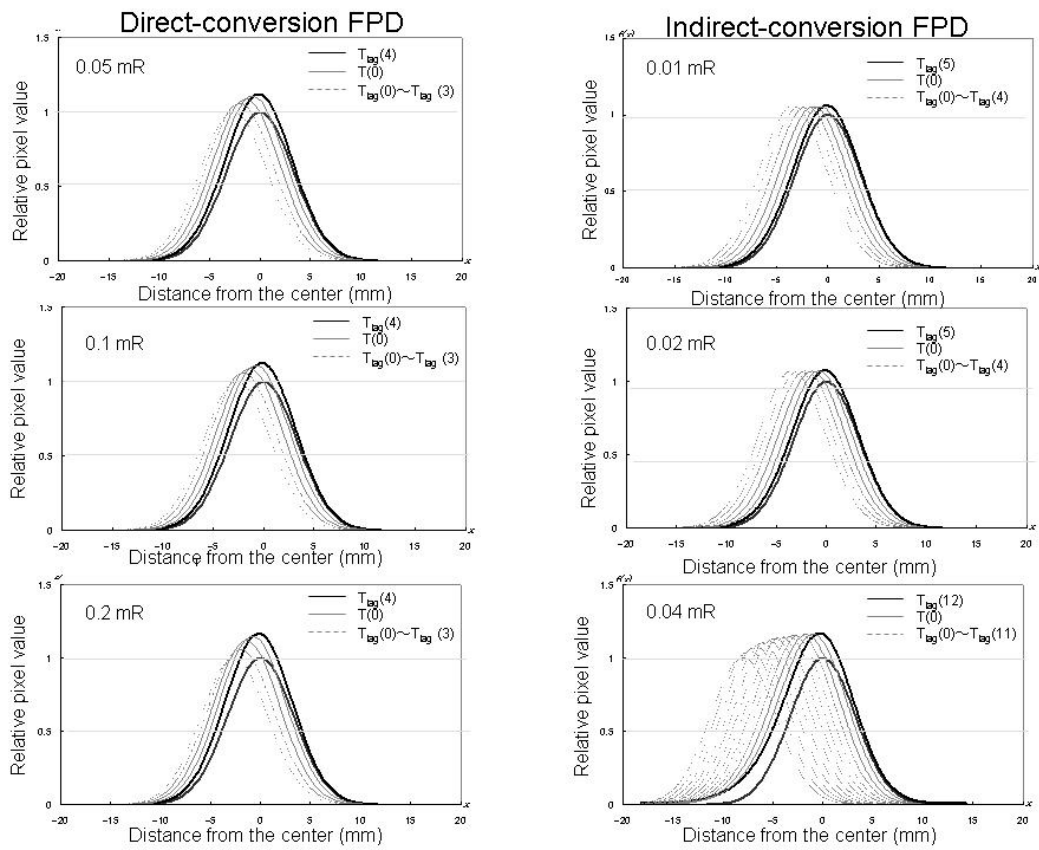target. (b) A real target cut out from a real radiograph.

Fig. 3 Profile curves of a target with image lag at each dose level in the case of a digital phantom simulating a lung tumor 1 cm in diameter. $T(0)$ means a target without lag, which is equivalent to a static target moving at 10 mm/s.
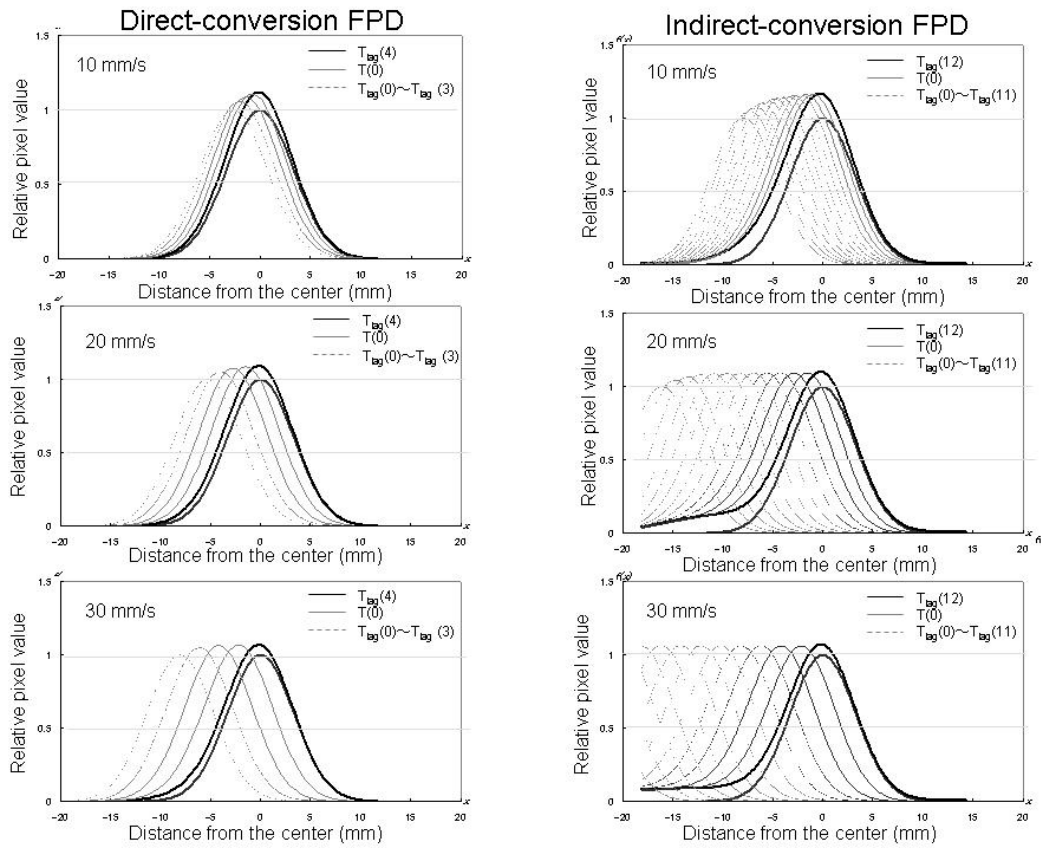
Fig. 4 Profile curves of a target with image lag at each target speed in the case of a digital phantom simulating a lung tumor 1 cm in diameter. $T(0)$ means a target without lag which is equivalent to a static target at reference dose levels, 0.2 mR in direct-conversion type and 0.04 mR in indirect-conversion type.
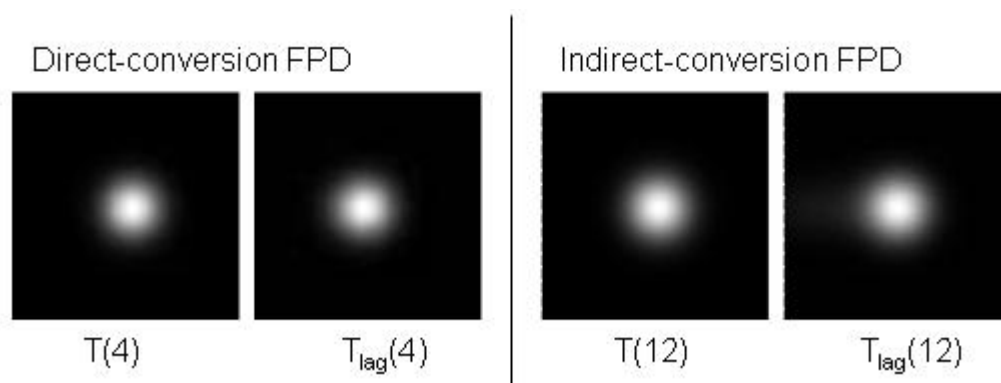
Fig. 5 Simulation target with and without image lag. $T_{lag}(n)$ means a target with lag, and $T(n)$ means a target without lag, which is equivalent to a static target.
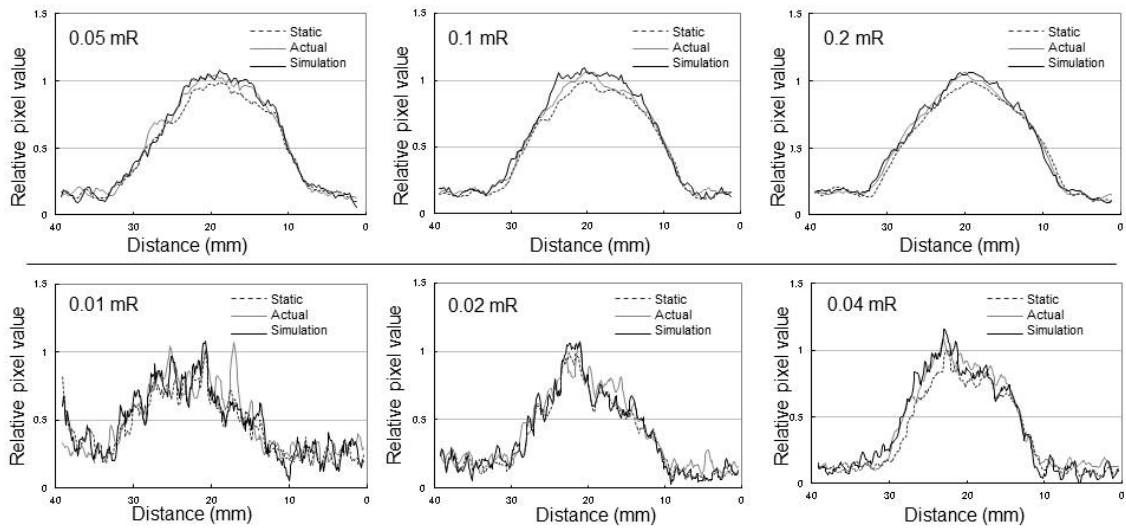
Fig. 6 Profile curves measured horizontally across actual static and moving targets and

a simulated motion target, obtained at three different dose levels (Upper:

direct-conversion FPD; lower: indirect-conversion FPD). The target speed was set at 10
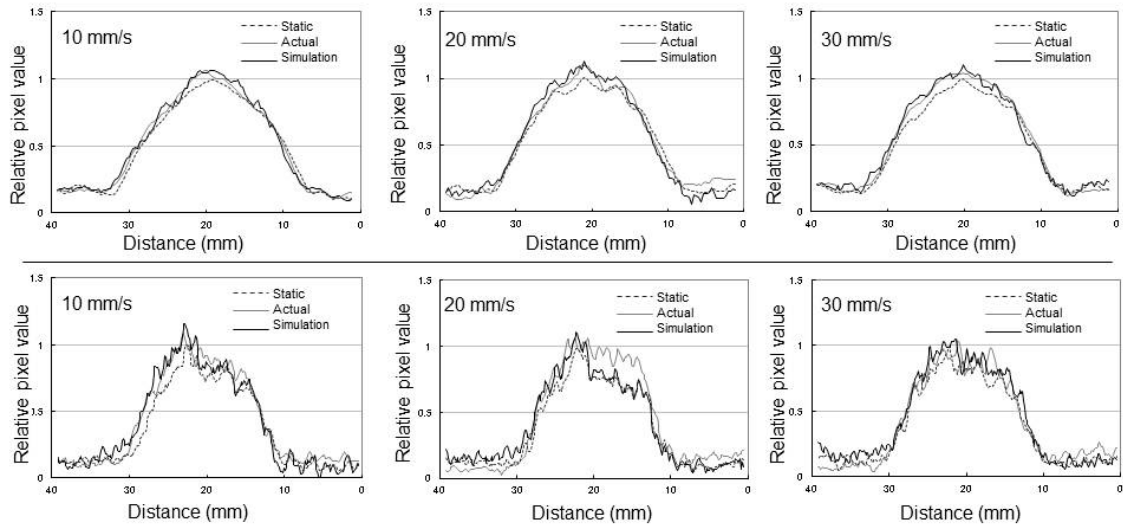
mm/s.

Fig. 7 Profile curves measured horizontally across actual static and moving targets and

a simulated motion target obtained at imaging rates of (a) 10 mm/s, (b) 20 mm/s, and (c)

30 mm/s (Upper: direct-conversion FPD; lower: indirect-conversion FPD). The exposure

dose was set at reference dose levels, 0.2 mR in direct-conversion type and 0.04 mR in

indirect-conversion type.